Molecular Crystals and Liquid Crystals Science and Technology. Section A. Molecular Crystals and Liquid Crystals
Publication details, including instructions for authors and subscription information:
http://www.tandfonline.com/loi/gmcl19

Alignment of Nematic Liquid Crystal(5CB) on the Treated Substrates: Characterization of Orientation Films, Generation of Pretilt Angles, and Surface Anchoring Strength

D. S. Seo [a] , H. Matsuda [a] , T. Oh-ide [a b] & S. Kobayashi [a]
[a] Division of Electronic and Information Engineering, Faculty of Technology, Tokyo University of Agriculture and Technology, 2-24-16 Nakamachi, Koganei, Tokyo, 184, Japan
[b] Production Technology Research Center, Ricoh Co. Ltd., Atsugi, Kanagawa, 243-02, Japan
Version of record first published: 24 Sep 2006.

To cite this article: D. S. Seo , H. Matsuda , T. Oh-ide & S. Kobayashi (1993): Alignment of Nematic Liquid Crystal(5CB) on the Treated Substrates: Characterization of Orientation Films, Generation of Pretilt Angles, and Surface Anchoring Strength, Molecular Crystals and Liquid Crystals Science and Technology. Section A. Molecular Crystals and Liquid Crystals, 224:1, 13-31

To link to this article: http://dx.doi.org/10.1080/10587259308032475

Mol. Cryst. Liq. Cryst., 1993, Vol. 224, pp. 13–31
Reprints available directly from the publisher
Photocopying permitted by license only

Printed in the United States of America

Alignment of Nematic Liquid Crystal(5CB) on the Treated Substrates: Characterization of Orientation Films, Generation of Pretilt Angles, and Surface Anchoring Strength

D.-S. SEO, H. MATSUDA, T. OH-IDE† and S. KOBAYASHI

Division of Electronic and Information Engineering, Faculty of Technology, Tokyo University of Agriculture and Technology, 2-24-16 Nakamachi, Koganei, Tokyo 184, Japan

(Received February 28, 1992)

This article provides a review on the experimental aspects of the alignment of nematic liquid crystal (NLC) in the pretilted homogeneous form in the sandwich cells; most of the contents of this paper are the results of research done by the authors in these few years. For simplicity and convenience, we used nematic liquid crystal (5CB) only; however, we have explored several polymer orientation films such as alkylbranched or alkylbranchless polyimide (PI), PI-Langmuir-Blodgett (LB) films, and those of polypyrrole. All these films were rubbed prior to assemble the cells except for some cases of PI-LB films. These films were characterized in terms of the atomic force microscope (AFM) observation and the optical retardation that are induced by the rubbing or unidirectional pulling up of the substrates in the LB process. Aligning capabilities of these orientation films for 5CB have been evaluated in terms of the texture of the NLC media, generation of pretilt angles, and temperature dependence of the anchoring strength (energies). Some results of this investigation is thought to partially contribute to provide several practical techniques for LCD technologies and to have some understanding the complicated surface anchoring phenomena.

Keywords: polyimide (PI) films, PI-Langmuir-Blodgett (LB) films, rubbing strength, optical retardation, pretilt angle, atomic force microscope (AFM), extrapolation length, polar anchoring energy

1. INTRODUCTION

The surface alignment or orientation of liquid crystal (LC) is of an interesting and important issue of the LC science and technology viewpoints.[1,2] The basic molecular conformations of the aligned LCs in a sandwich cell are the so called homeotropic or homogeneous ones. The former stands for an LC conformation in which the director takes normal direction to the substrates, while the latter horizontal. In both cases, it is necessary to give a pretilt angle in order to avoid the creation of

†On leave from Production Technology Research Center, Ricoh Co. Ltd., Atsugi, Kanagawa 243-02, Japan

the disclinations. This means that LC molecules have to be aligned to form a monodomain that accompanies a finite off angle from the vertical or horizontal (planar) direction in reference to on the substrate surface. For the homeotropic alignment of LC, it is practical to make use of oblique evaporation technique of SiO or that of the stacking of amphiphilic molecules.[1] While, the homogeneous alignment of LC can also be made by using obliquely evaporated SiO[1] or rubbed polymer, in particular polyimide (PI) films.[3–7]

The latter are widely utilized in the LCD industry and scientific research. Recently we showed the effective utility of the as stacked and rubbed PI-LB films[8–13] and rubbed polypyrrole (PP)[14,15] for their very thinness and electrical conductivity that are effective to discharge the accumulated charges in the interfacial regions of a cell through an external circuit. The accumulation of these charges degrade the EO performance of LCDs. Discussion on the polypyrroles is not made in this paper.

We have explored various spin coated and rubbed PI[5–7] and PI-LB films.[9–13] In order to characterize the orientation of these films we have done atomic force microscope (AFM) observation on the morphologies of the surfaces together with 2D fourier spectra and the measurements of the optical retardation occurring on the surface of the oriented film due to the rubbing.[16] The aligning capabilities of these oriented films for NLC(5CB) have been assessed in terms of their microphotographic texture, generation of the pretilt angles, and the temperature dependence of the anchoring energies. Among them, the generation of a high pretilt angle by the rubbing on the oriented film is one of the most important

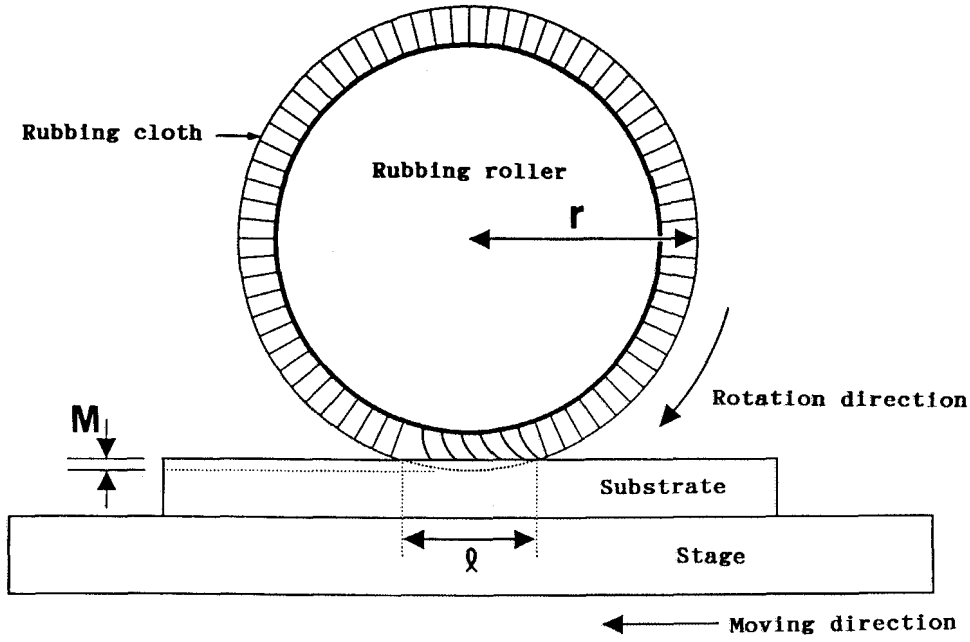

FIGURE 1 A schematic diagram of the rubbing machine. The depth of the deformed region of the rubbing cloth designated by M due to the contact is an important parameter characterizing the rubbing strength.

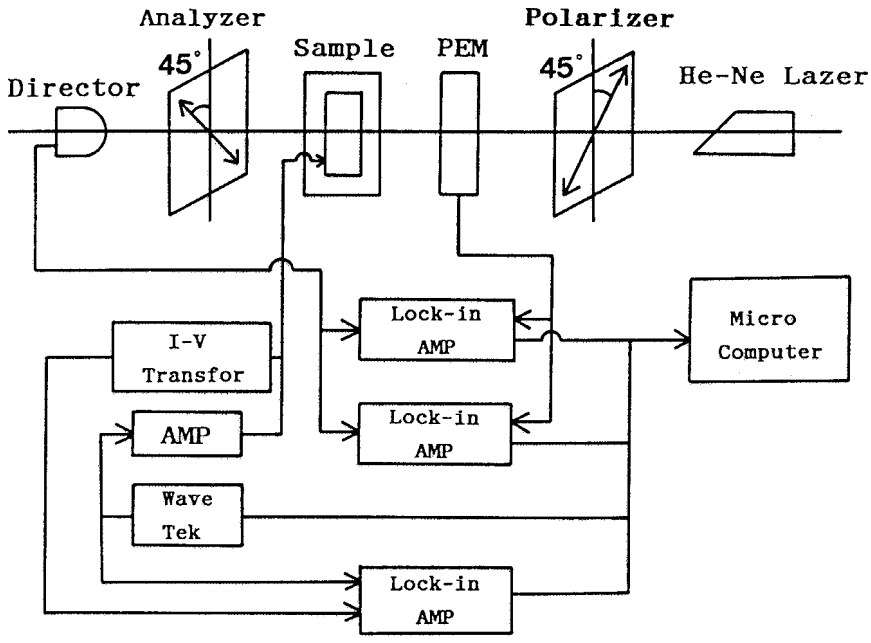

FIGURE 2 Experimental setup for measuring the optical retardation (R) and electrical capacitance (C).

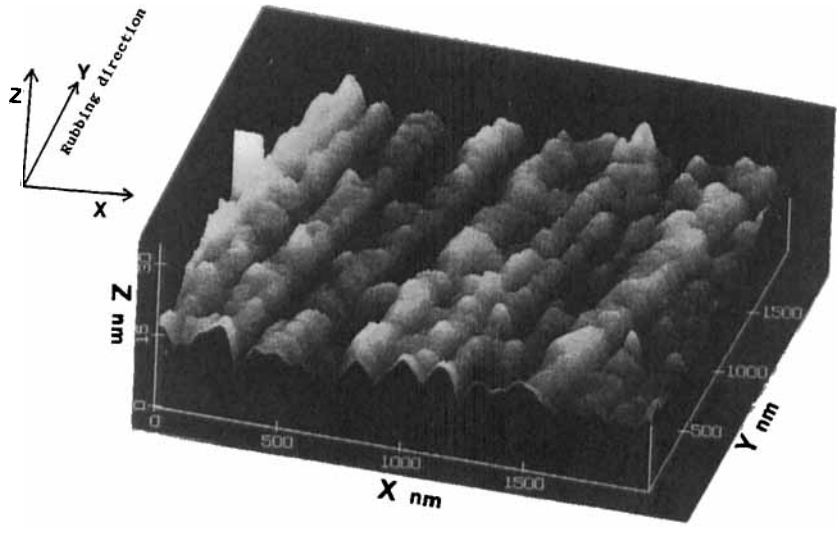

(a)

FIGURE 3 An AFM image of the rubbed PI(2) film for a medium rubbing strength (RS = 273 mm) with an atomic force microscope (AFM). (a) is surface morphology; (b) is 2D power spectrum of the fourier analysis. See Color Plate I.

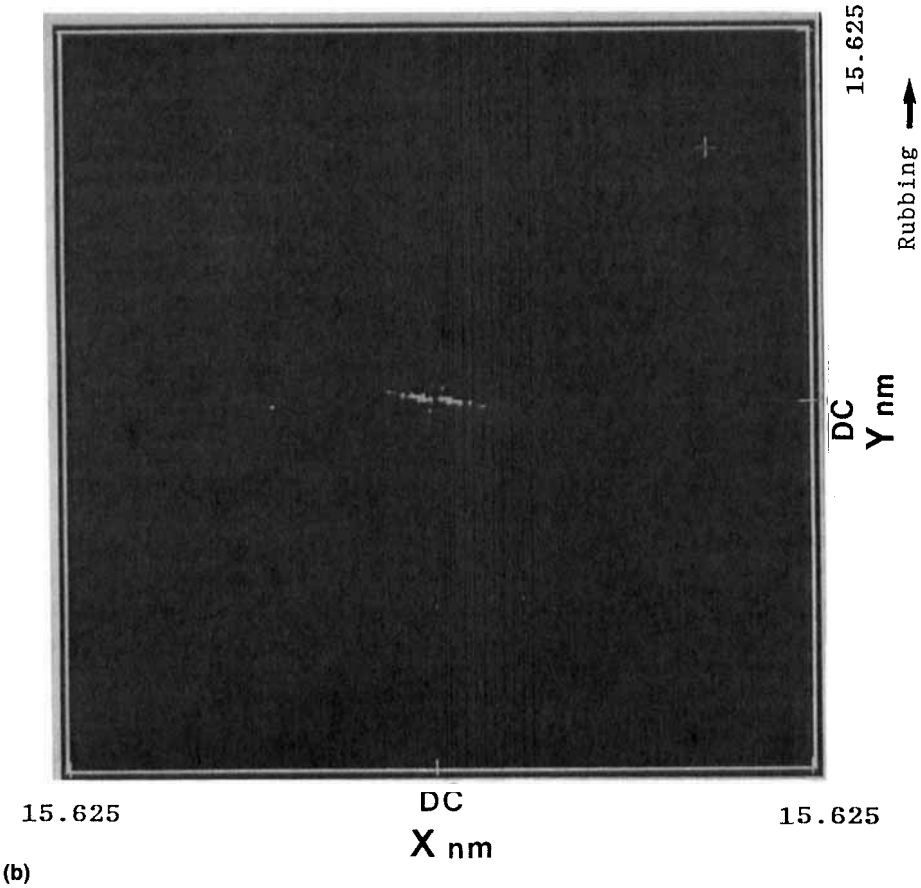

FIGURE 3 (*Continued*) See Color Plate I.

issues in the LCD industry. The technique for realizing defect free super twisted nematic (STN) LCDs was proposed and demonstrated by the authors group using appropriately rubbed alkyl-branched PI films.[3–7] In the course of this research we controlled the rubbing strength which has been defined in Reference 5.

2. EXPERIMENTAL

2.1 Samples

The samples used in our research were fabricated by using different kinds of polyimide films which were prepared either by means of spin-coating or LB technique. Their code names and features are as follows:

PI(1)—it consists of molecules with trifluoromethyl moieties and containing a cyclobutane part; it is featured by the small electrical polarization.
PI(2)—alky-branched and with cyclobutane, medium polarization.

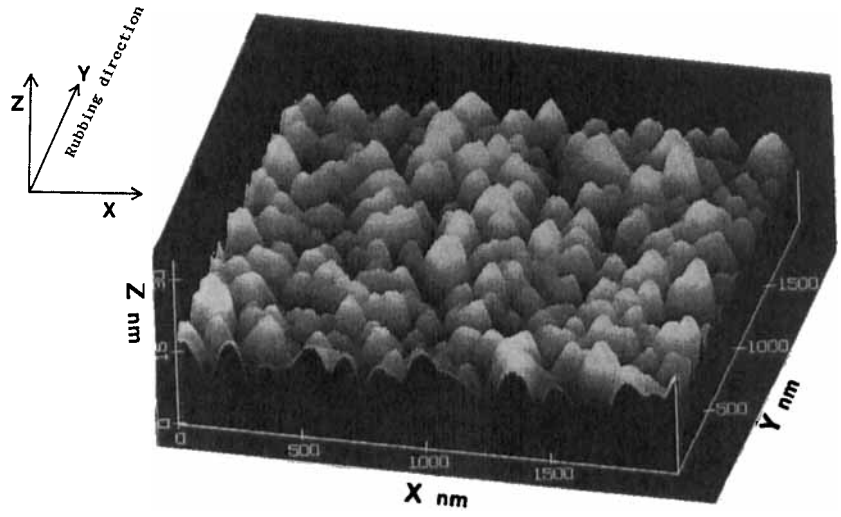

(a)

FIGURE 4 An AFM image of the rubbed PI(3) film for a medium rubbing strength (RS = 273 mm) with an atomic force microscope (AFM). (a) is surface morphology; (b) is 2D power spectrum of the fourier analysis. See Color Plate II.

PI(3)—alkyl-branchless and with cyclobutane, the largest polarization.
PI(4)—alkyl-branchless and with cyclopentane, medium polarization.

The aforementioned first three PI films were spin coated on indium-tin-oxide (ITO) coated glass plates and then they were polyimidized at 250°C for one hour. The PI-LB films were fabricated using precursor for PI(1), PI(2), and PI(4). The PI-LB films were prepared first by synthezing polyamic acids (by attaching alkyl-amines to the precursor which was supplied by Japan Synthetic Rubber), the acids were stacked on the ITO glass then they are chemically polyimidized, using chemical polyimidation method. The PI-LB films prepared were Y-type of 9 molecular layers.

The rubbing was done with a machine whose drum was wrapped with a nyloncloth (Y_o-15-N, from Yoshikawa Chemical Industries Co. Ltd.). The nematic liquid crystal (NLC) used in the experiment was 4-cyano-4′-n-pentylbiphenyl(5CB) and it was aligned to form homogeneous monodomain medium by antiparallel rubbing in a sandwich cell. All sample cell had an LC layer of 60 ± 0.3 μm thick.

2.2 Rubbing strength (RS)

The cross-sectional view of the rubbing machine is shown in Figure 1. In this research, we adopted the following expression for the rubbing strength RS:

$$\mathrm{RS} = NM(2\pi rn/v - 1), \tag{1}$$

where N is the number of the repeated times for the rubbing (usually $N = 1$ in

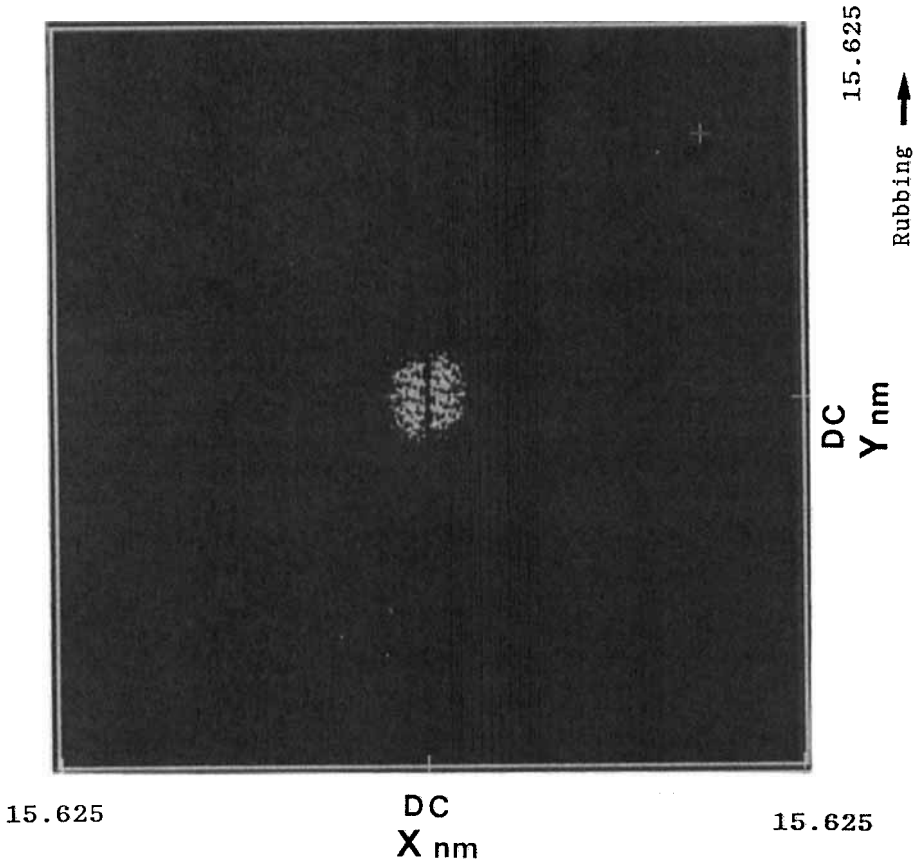

FIGURE 4 (*Continued*) See Color Plate II.

our work), M is the depth of the deformed fibers of the cloth due to the pressed contact (mm), n is the rotation rate of the drum (1000/60(S^{-1})), v is the translating speed of the substrate (7.0 mm/s), and r is the radius of the drum.

We adopted the parameter M as the most important adjustable one to control the rubbing strength while the other parameters were kept constant. The actual rubbing work W per unit area may be proportional to the RS as $W = a \cdot \mathrm{RS}$, where a is the proportional coefficient as a function of the kinetic friction and the energy transfer ratio between two contacting surfaces and so forth.[5]

2.3 Pretilt angle measurement

For measuring pretilt angles we used the magneto capacitive null method for the values above 10 degrees[17] and method of crystal rotation below 10 degrees[18]; the measurements were done at room temperature.

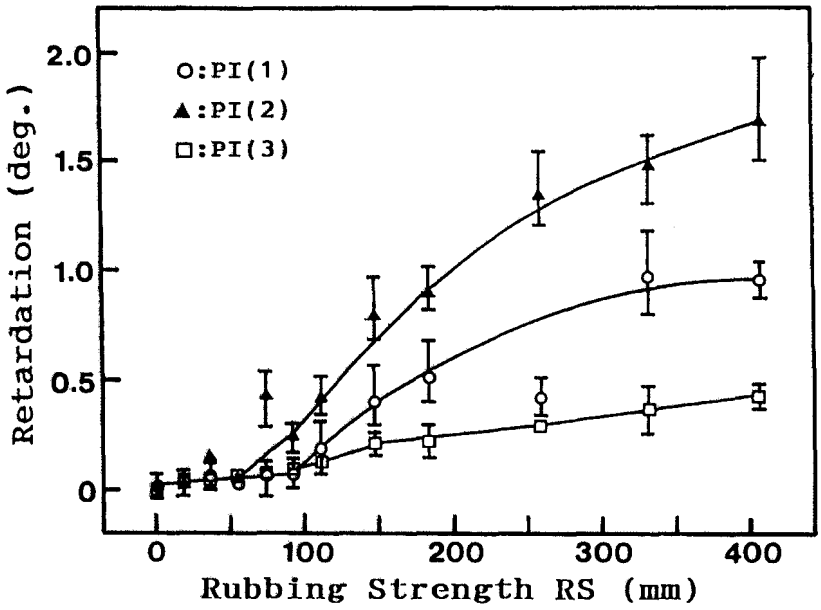

FIGURE 5 The optical retardation induced by the rubbed PI(1) through PI(3) films as a function of rubbing strength.

2.4 Observation of the surface structure

The observations of the surface morphologies for both surfaces of ITO films coated on the glass plates and the polymer films coated or stacked on the substrates were done with an atomic force microscope (model Nano Scope II).

2.5 Optical retardation on the rubbed PI films

The optical retardation occurring on the surfaces of the rubbed PI films were measured for the rubbing strength with an instrument which will be explained in the next subsection.

2.6 Measurement of polar anchoring energy

In order to measure the anchoring strength (energy), we used the "high electric-field technique."[19,20] Figure 2 shows the experimental setup for measuring the optical retardation (R) and electrical capacitance (C).[21] The light source is a He-Ne laser (632.8 nm) with 2 mW output power. The measurement system of the optical retardation consists of a polarizer, an acoustic modulator, and an analyzer and the output signal is detected by a photodiode. The electric capacitance of the LC cell is obtained by measuring the out-of-phase component of the current by changing the voltage applied to the cell.

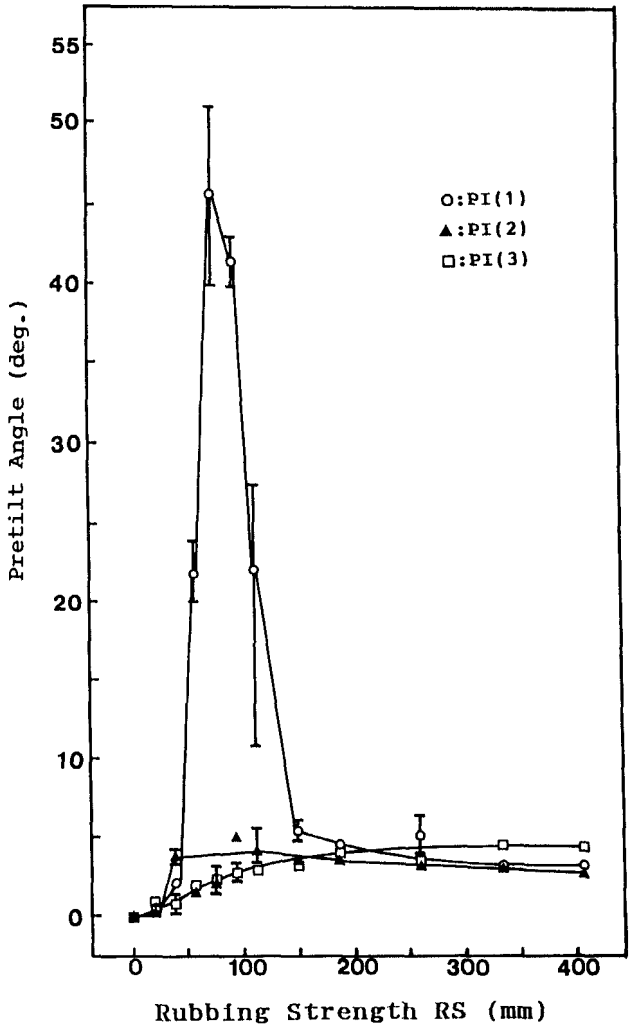

FIGURE 6 The generation of the pretilt angles for 5CB aligned in the cells with the rubbed PI(1) through PI(3) films as a function of rubbing strength.

We evaluated the extrapolation length (de) by using the relationship between the measured values of the electric capacitance (C) and the optical retardation (R):

$$\frac{R}{R_o} = \frac{I_o}{CV} - \frac{2d_e}{d} \quad \text{when} \quad V > 6V_{\text{th}}, \tag{2}$$

where I_o is a proportional constant depending on the LC materials; V and d stand for the applied voltage and the LC medium thickness, respectively.

We determined the polar anchoring energy A from the following relation:

$$A = K/d_e \tag{3}$$

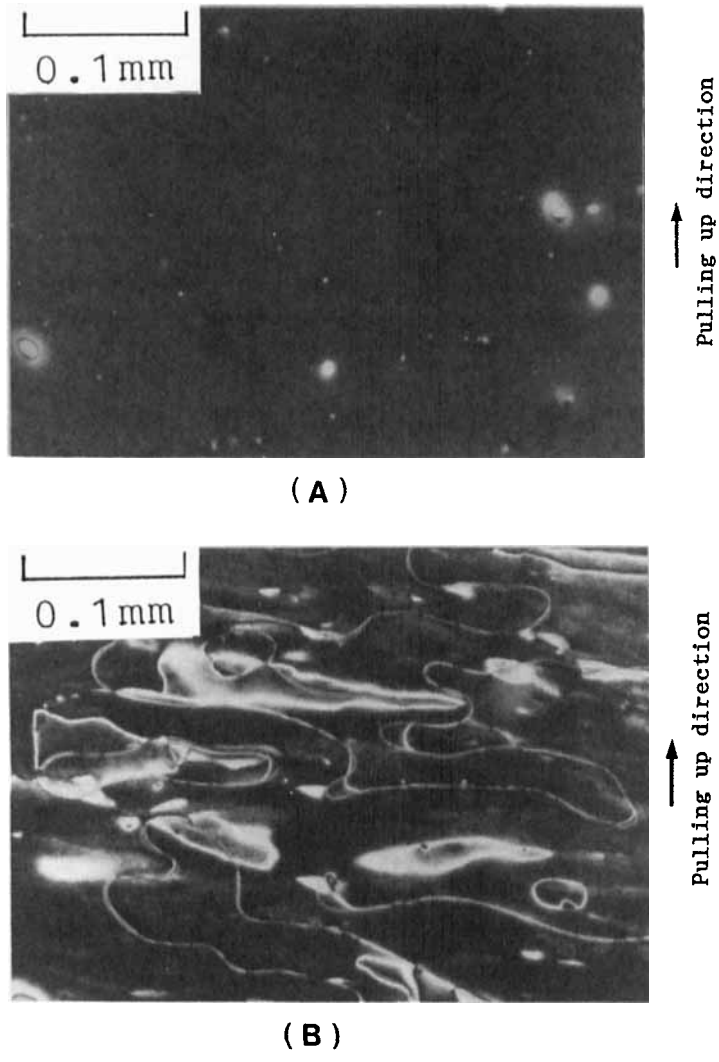

FIGURE 7 Microphotographs of the textures for 5CB under cross-nicols. (a) is for a cell with the Y-type PI(4)-LB films of 9 layer; (b) is for that prepared with the Z-type PI(4)-LB films of 9 layer. See Color Plate III.

where K is the effective elastic constant which is given as $K = K_1 \cos^2\theta_p + K_2 \sin^2\theta_p$, whereas K_1, K_3, and θ_p stand for the elastic constants of the splay, bend deformation, and the pretilt angle, respectively.

3. RESULTS AND DISCUSSION

3.1 Observation of the surface morphologies of rubbed PI films

Figure 3(a) shows an example of the surface morphology of the rubbed PI(2) film for medium rubbing strength (RS = 273 mm) with an atomic force microscope (AFM). While, Figure 3(b) shows the 2D power spectrum of the fourier analysis

TABLE 1

Rubbing strength dependence of the pretilt angles in nematic liquid crystal (5CB) cells with the orientation of the films on the bare ITO and those of PI-LB.

Samples	Pretilt Angle(deg.)	
	Rubbing Strength RS(mm)	
	0	189
ITO		0
PI(1)-LB	0.2	1.7
PI(2)-LB	0.2	2.5
PI(4)-LB	0	0.9

of the same film; an anisotropy in the structure is observed along the perpendicular direction to the rubbing direction.[22,23]

On the other hand, no such a distinct morphologies is seen for the rubbed PI(3) film that were rubbed at medium RS (RS = 273 mm) as shown in Figure 4(a). In corresponding to this situation no anisotropy in the surface structure is observed in this case (Figure 4(b)).[22,23]

However, according to the texture observations both films were shown to be well capable of aligning the NLC.

3.2 *Optical retardation induced by the rubbing*

The optical retardation induced rubbing done on the rubbed PI(1) through PI(3) films due to rubbing as a function of the RS (mm) as shown in Figure 5.[5,6] The optical retardation increase with the RS (mm) for different three rubbed PI films. It is considered that the optical retardation may be induced by a plastic flow of the polymer in its surface region in terms of the unidirectional alignment of the main chains of the polymer.

3.3 Generation of pretilt angles

Figure 6 shows the generation of the pretilt angles for NLC(5CB) aligned in the cells with different kinds of the rubbed PI films as a function of the RS (mm).[5,6] The cell with the rubbed PI(1) films shows a giant peak reaching about 51 degrees for weak RS (RS = 76.5 mm) and hereafter the pretilt angle decreases to the level

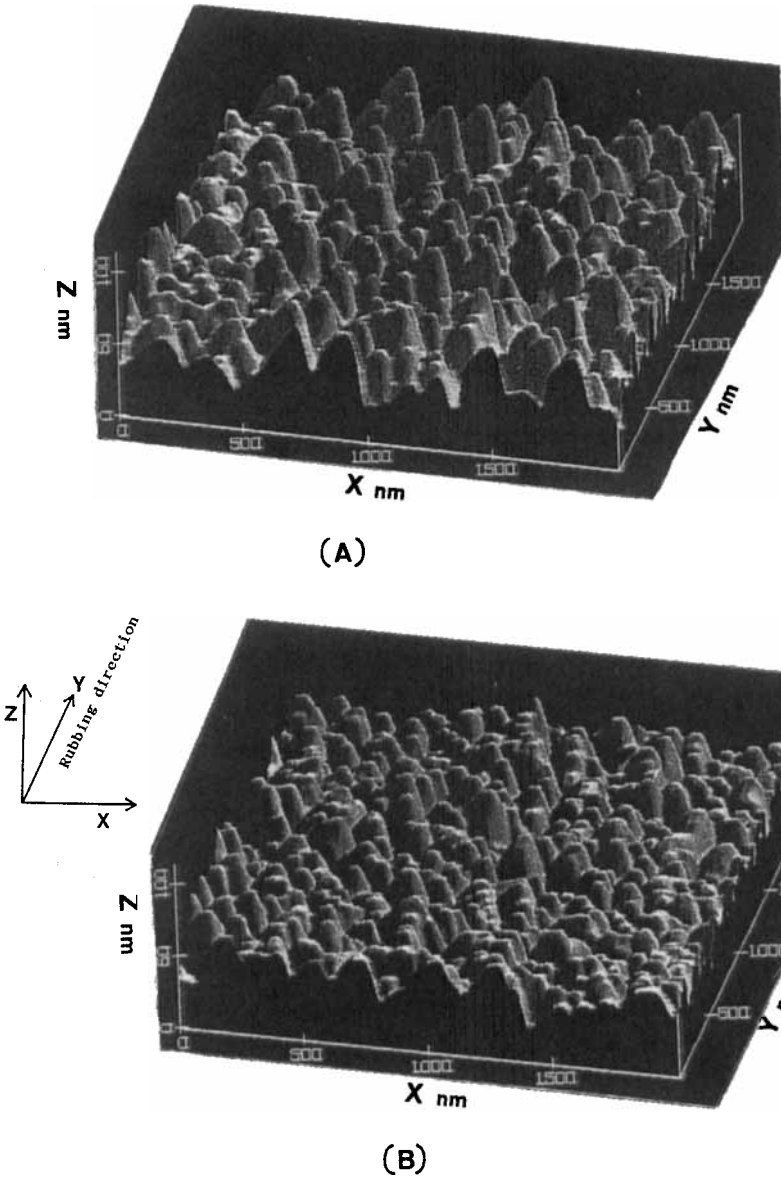

FIGURE 8 AFM images of the ITO films. (a) is bare ITO films; (b) is rubbed ITO films (RS = 189 (mm)). See Color Plate IV.

off to 4 degrees or less. The formation of this kind of high pretilt angles is attributable to the existence of trifluoromethyl moieties on the worked PI surfaces. This material is useful for generating a high pretilt angle above 5 degrees. The pretilt angle for the rubbed PI(2) films having alkylbranches show a rapid rise in the weak rubbing region and it tends to 3.5 degrees; the steric interaction between the LC and alkyl-branches is thought to be the origin of the pretilt. While, the pretilt angle

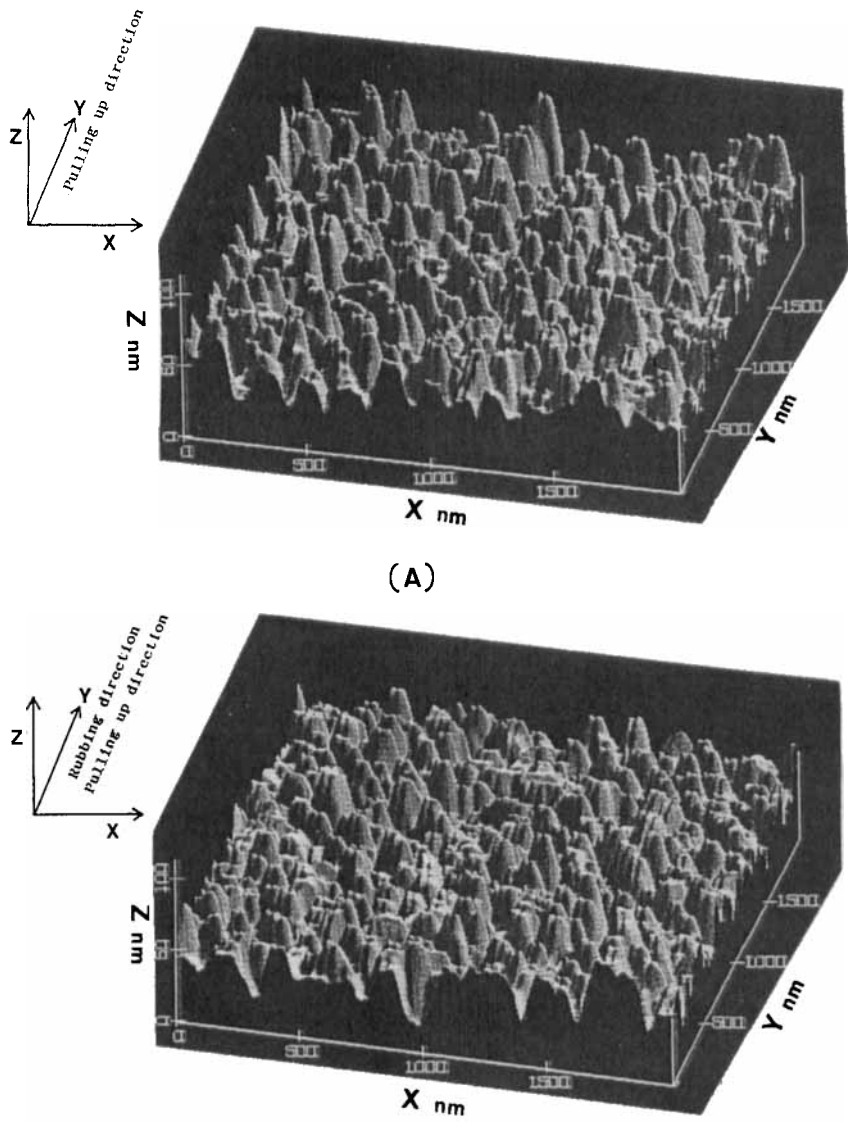

FIGURE 9 AFM images of the PI(1)-LB films. (a) is for the as stacked PI(1)-LB films; (b) is for the rubbed PI(1)-LB films (RS = 189 (mm)). See Color Plate V.

for the rubbed PI(3) films increases with the RS from a small value then it tends a saturation toward about 4.5 degrees. This unique behaviour may be attributed to the molecular structure of this material for high polarization.

Generally, the creation of the pretilt angles may be attributable to the following mechanisms of interaction between LC and substrate such as steric interaction, that of dispersion force and dipole-dipole type. The existence of the alkylamine

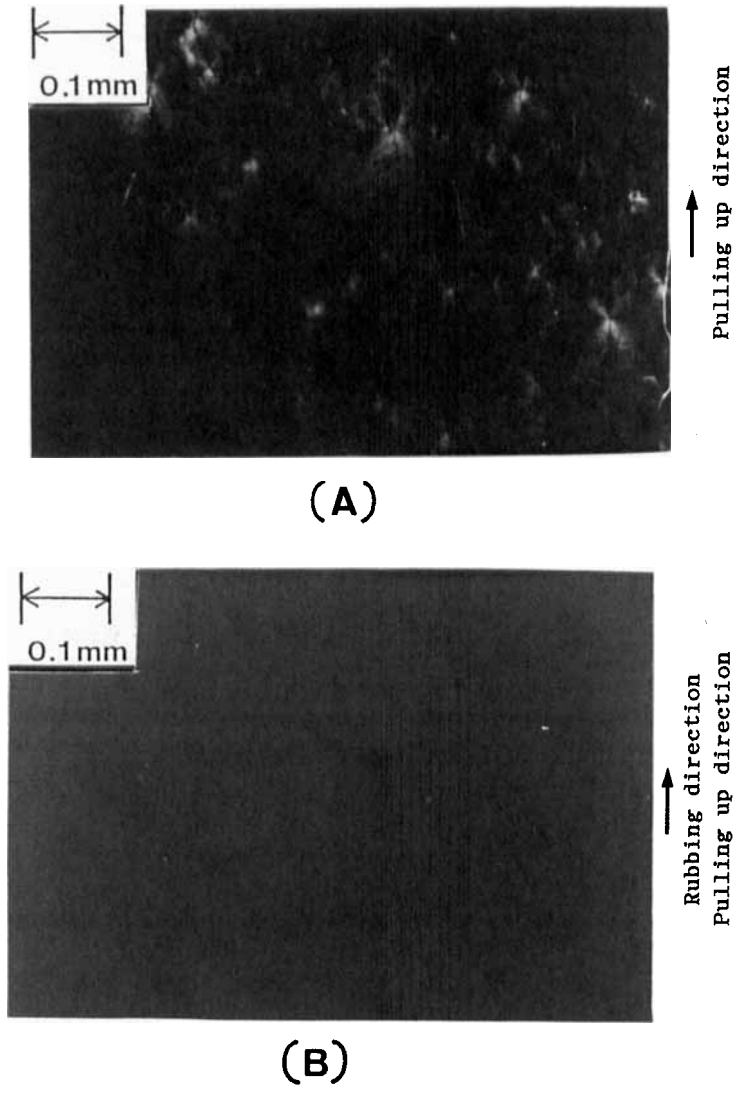

FIGURE 10 Microphotographs of textures for 5CB under cross-nicols. (a) is with the as stacked PI(4)-LB films; (b) is with the rubbed PI(4)-LB films (RS = 189 (mm)). See Color Plate VI.

and trifluoromethyl moieties on the surface make them strong hydrophobic that controls the alignment of LCs; the alkyl-branches may play a role in the steric interaction; the rubbing may create a slanted easy axis off from the surface that may induce a pretilt angle owing to the dispersion force; stick slip type work on the rubbed surface may create a repeated-slanted structure on the surface. Depending on the nature of the LC and orientation of the films, one of the above mentioned mechanisms may play a dominant role in the creation of the pretilt.

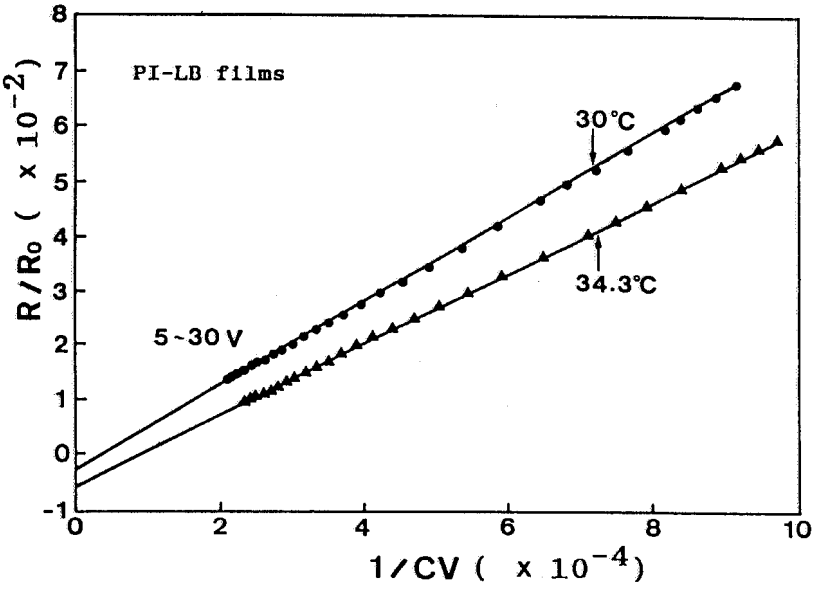

FIGURE 11 The plots of R/R_o versus $1/CV$ on a cell with the as stacked Y-type PI(4)-LB films (9 layer) at different two temperatures.

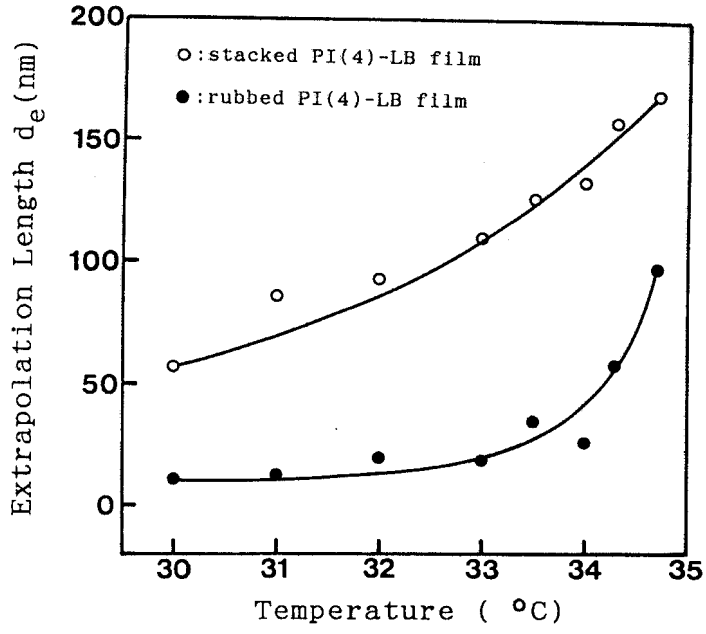

FIGURE 12 Temperature dependence of the extrapolation length (d_e) for 5CB on the as stacked and rubbed PI(4)-LB films for medium rubbing strength.

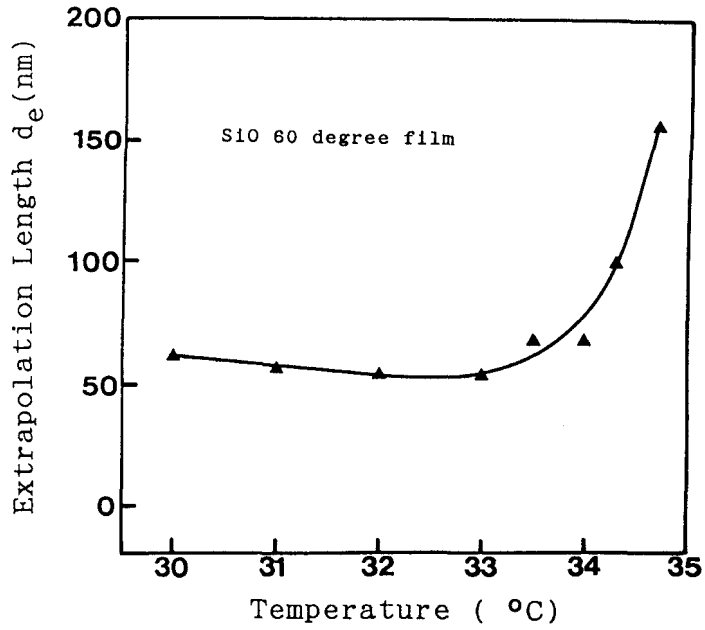

FIGURE 13 Temperature dependence of the extrapolation length (D_e) for 5CB on the oblique evaporation SiO 60 degree film.

3.4 Alignment of NLC on the as stacked and rubbed PI-LB films

Figure 7 shows the microphotographs of the textures of nematic liquid crystal (5CB) aligned on the as stacked Z-type and Y-type PI(4) films having 9 molecular layers.[9] It is shown that the as stacked Y-type PI(4)-LB films having 9 molecular layers are capable of aligning the NLC(5CB) to form an excellent uniform monodomain medium; while, the Z-type yield many defects as shown in Figures 7(a) and (b).

Table 1 compares the generation of the pretilt angles aligned on the various kind of stacked and rubbed PI-LB films of the Y-type with 9 molecular layers. It is shown that the pretilt angles are generated by the rubbing in the cells with the rubbed PI(1)-LB and PI(2)-LB films, while no pretilt angle is observed for the rubbed bare ITO films and rubbed PI(4)-LB films.[10]

3.5 Observation of surface morphologies on the as stacked and rubbed PI-LB films

Figure 8 shows AFM images of the bare ITO films in the field of view 2000 nm in the X and Y directions, where Figure 8(a) and (b) show the surface morphologies of the bare ITO films and the rubbed ITO films for a medium RS (mm) with a nylon cloth, respectively.[10] These photographs were taken as references to the succeeding experiments. Also some irregular structure having about 40 nm height are seen.

Figure 9(a) and (b) show the AFM images of the as stacked PI(1)-LB films of the Y-type with 9 molecular layers deposited on the ITO films and the rubbed PI(1)-LB films, respectively.[10] The direction of the rubbing is the Y direction in

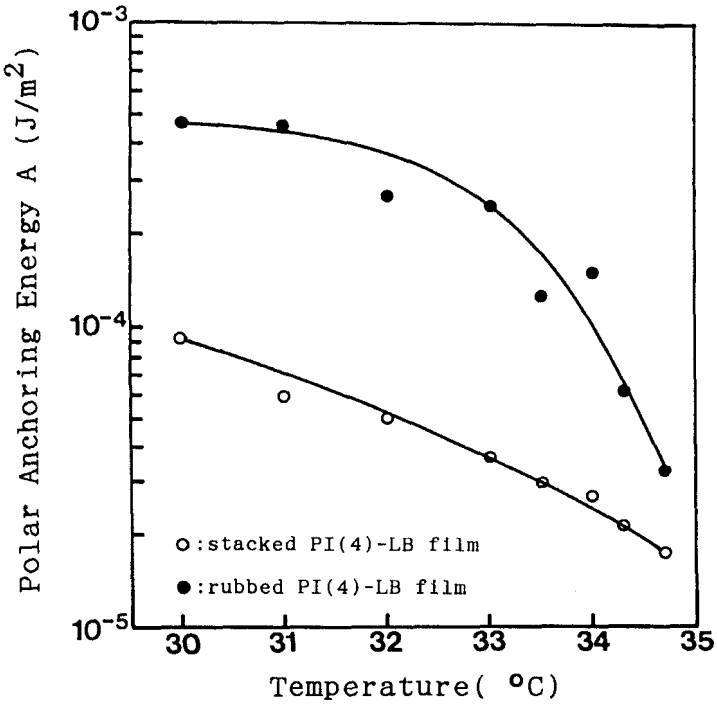

FIGURE 14 Temperature dependence of the polar anchoring energies (A) for 5CB aligned as the as stacked and rubbed PI(4)-LB films for medium rubbing strength.

Figure 9(b). No grooves for the rubbed PI-LB(1) films are observed in the surface morphology of Figure 9(b).

Due to the thinness of the PI(1)-LB film (about 4 nm) it may be natural that the morphology of the stacked surface is almost the same as that of the bare ITO films. However, it is recognizable that the surfaces are flattened due to the rubbing on the rubbed PI-LB films as shown in Figures 8(b) and 9(b).

3.6 Textures of aligned NLC on PI-LB films

Figure 10 shows the microphotographs of the textures for nematic liquid crystal (5CB) in the sample cells with the as stacked and rubbed PI(1)-LB films of the Y-type having 9 molecular layers, respectively. It becomes evident that the rubbing makes the texture more uniform.[10] The fact that the NLC is aligned very well on the as stacked PI-LB films and that there are no grooves suggests that the existence of the parallel grooves[24] are not the necessary condition for the LC alignment.

3.7 Anchoring strength (energy) for 5CB aligned on the various orientation films

Regarding the polar anchoring energy (A) for NLC(5CB), it is easy to measure it on a cell with obliquely evaporated SiO since the anchoring energy is small enough (about 10^{-4} (J/m^2))[6,9,19,20] due to the roughness of the SiO films; however, the A for a rubbed PI film is about 10^{-3} (J/m^2) or more, so it is rather too strong to

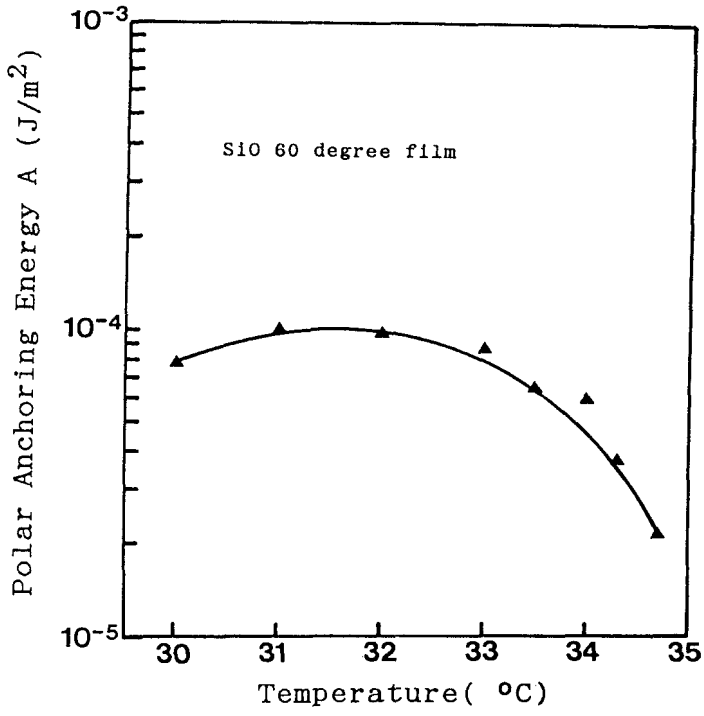

FIGURE 15 Temperature dependence of the polar anchoring energies (A) for 5CB aligned on the obliquely evaporated SiO (60 degrees) films as a function of temperature.

measure. Recently, however, we succeeded in measuring it by adjusting the rubbing intensity.[21]

The values of A for the existing PI-LB films lies between two extreme cases mentioned above.

Figure 11 shows an example of the plot R/R_o versus $1/CV$ on a cell with the as stacked PI(4)-LB films with Y-type of 9 layers at different temperatures. The extrapolation length d_e are obtained from the intersection of the straight lines with the ordinate axis.

Figure 12 shows the temperature dependence of the extrapolation length d_e for NLC(5CB) aligned on the as stacked and rubbed PI(4)-LB films for medium RS (RS = 189 mm); the extrapolation lengths for both films are shown to increase with temperature and tend to diverse approaching of the N-I (nematic-isotropic) transition point (T_{NI} = 35.3°C). It is demonstrated that the rubbing contributes to reduce the extrapolation length. For a comparison, we measured the extrapolation length for 5CB aligned on the oblique evaporation SiO films with 60 degrees as a function of temperature which is shown in Figure 13. It exhibits an increase with the increase of the temperature.

From the above results, we determined the polar anchoring energy by using Equation (3). Figure 14 shows the polar anchoring energies for 5CB aligned on the as stacked and rubbed PI(4)-LB films for medium RS as a function of temperature. It is shown that both of the polar anchoring energies decrease with the

increase of the temperature and it becomes almost zero at the N-I transition. The polar anchoring energies for 5CB are 9.4×10^{-5}, and 4.75×10^{-4} (J/m^2) at 30°C aligned on the as stacked and rubbed PI(4)-LB films, respectively. The polar anchoring energies are shown to increase with the rubbing. We consider that this increase in the polar anchoring energy may be originated from the increase of the surface order parameter due to the rubbing.[13]

Figure 15 shows the polar anchoring energies for 5CB aligned on the obliquely evaporated SiO 60 degree films as a function of temperature. The polar anchoring energy also decreases with temperature. The polar anchoring energy for 5CB is 7.9×10^{-5} (J/m^2) at 30°C; this value is almost equivalent to that for the as stacked PI(4)-LB films.

4. CONCLUSION AND SUMMARY

We have investigated the surface morphologies of the films for various surface orientation with an atomic force microscope (AFM) for the first time. These films include the rubbed PI films, bare and rubbed ITO films, as stacked and rubbed PI-LB films. Besides, we also conducted the generation of the pretilt angles for nematic liquid crystal (5CB) aligned on three kinds of the rubbed polyimide (PI) films as a function of rubbing strength (RS) whose magnitude is monitored by the induced optical retardation due to the rubbing. Furthermore, we measured the polar anchoring energy for 5CB aligned on the as stacked and rubbed PI-Langmuir-Blodgett (LB) films as a function of temperature.

The grooves are observed on the rubbed PI films with alkyl-branches for medium RS (mm), while no grooves are observed on the rubbed alkyl-branchless PI films. On the other hand, both of the PI films are well capable of aligning NLC.

The pretilt angles for 5CB are generated in the media aligned on three kinds of rubbed PI films depending on the RS (mm). We observed a giantic high pretilt angle in a cell with weakly rubbed PI films containing trifluoromethyl moieties then it gradually tends to level off to 4 degrees; a rapid increase in the pretilt angle and a saturation to about 5 degree are obtained for the rubbed PI films having alkyl-branches; starting from zero degree and a gradual saturation toward about 4.5 degrees are obtained with the rubbed PI films with alkyl-branchless.

The microphotographic textures of NLC(5CB) aligned on the as stacked Y-type PI-LB films of 9 layers are fairly uniform in comparison with the as stacked Z-type PI-LB films.

No grooves are observed on the surface of the as stacked and rubbed PI-LB films of the Y-type having 9 layers. The surface morphologies are flattened by the rubbing. The origin of the alignment is thought to be attributable to the anisotropic dispersion force between the LC and PI-LB film. The microphotographs of the textures for 5CB are shown to become more uniform due to the rubbing done on the PI-LB film.

The polar anchoring energies between the 5CB and the as stacked and rubbed PI-LB films decrease with the increase of the temperature; and the polar anchoring energy in this system is shown to increase with the rubbing. This increase is thought to be originated from the increase of the surface order parameter due to the rubbing.

References

1. J. Cognard, *Mol. Cryst. Liq. Cryst. Supplement*, **1,** 1 (1982).
2. H. Yokoyama, *Mol. Cryst. Liq. Cryst.*, The 100th anniversary of the Liquid Crystal Research (S. Kobayashi, ed.), **265**, 269 (1988).
3. S. Kuniyasu, H. Fukuro, S. Maeda, K. Nakaya, M. Nitta, N. Ozaki and S. Kobayashi, *Jpn. J. Appl. Phys.*, **27**, 827 (1988).
4. T. Sugiyama, S. Kuniyasu, D.-S. Seo, H. Fukuro and S. Kobayashi, *Jpn. J. Appl. Phys.*, **29**, 2045 (1990).
5. D.-S. Seo, K. Muroi and S. Kobayashi, *Mol. Cryst. Liq. Cryst.*, **213,** 223 (1992).
6. D.-S. Seo and S. Kobayashi, 2nd Japan-Korea Joint Symposium on Information Display (October 31, 1991, in Sendai); IEICE Technical Report EID 91-49 (English), 15 (1991).
7. D.-S. Seo, S. Kobayashi and M. Nishikawa (submitted).
8. H. Ikeno, A. Ohsaki, M. Nitta, N. Ozaki, Y. Yokoyama, K. Nakaya and S. Kobayashi, *Jpn. J. Appl. Phys.*, **27,** 475 (1988).
9. D.-S. Seo, H. Maeda, H. Matsuda and S. Kobayashi, *Mol. Cryst. Liq. Cryst.*, **209,** 123 (1991).
10. D.-S. Seo, T. Oh-ide and S. Kobayashi, *Mol. Cryst. Liq. Cryst.*, **214,** 97 (1991).
11. D.-S. Seo, Y.-B. Yang and S. Kobayashi, 2nd Korea-Japan Joint Forum 91 Organic Thin Films (October 23–24, 1991, in Seoul), 10 (1991).
12. D.-S. Seo, H. Matsuda, K. Muroi, H. Yokoyama and S. Kobayashi, 17th Japanese Liquid Crystal Conference (September 23–25, 1991, in Sapporo), **2F116**, 42 (1991).
13. D.-S. Seo, K. Muroi, T. Isogami, H. Matsuda, S. Kobayashi and H. Yokoyama (submitted).
14. D.-S. Seo, S. Kobayshi and A. Mochizuki, *Appl. Phys. Lett.*, **60**(8), 1025 (1992).
15. D.-S. Seo and S. Kobayashi, IEICE Technical Report **EID 91-109** (Japanese), 7 (1992).
16. J. M. Geary, J. W. Goodby, A. R. Kmetz and J. S. Patel, *J. Appl. Phys.*, **62**(10), 4100 (1987).
17. L. Komitov, G. Hauck and H. D. Koswing, *Crys. Res. and Tech.*, **19**, 253 (1984).
18. T. J. Scheffer and J. Nehring, *J. Appl. Phys.*, **48**, 1783 (1977).
19. H. Yokoyama and H. A. van Sprang, *J. Appl. Phys.*, **57**, 4520 (1985).
20. H. Yokoyama, S. Kobayashi and H. Kamei, *J. Appl. Phys.*, **61**(9), 4501 (1987).
21. D.-S. Seo, Y. Iimura and S. Kobayashi, accepted for publication in Appl. Phys. Lett, in press (1992).
22. D.-S. Seo, T. Isogami, K. Muroi and S. Kobayashi, IEICE Technical Report EID **91-108** (Japanese), 1 (1992).
23. D.-S. Seo, T. Isogami, T. Oh-ide, K. Muroi, H. Matsuda, Y. Yabe, Y.-B. Yang, T. Bang, A. Mochizuki and S. Kobayashi, accepted for presentation in SID (May 17–22, 1992, in Boston).
24. D. W. Berreman, *Phys. Rev. Lett.*, **28**, 1683 (1972).